

# Solar Tower Power Plant Reliability Analysis using FORM method

Samir Benammar<sup>1</sup>, Abdellah Khellaf<sup>2</sup>

<sup>1</sup>(Laboratoire Energétique - Mécanique & Ingénieries (LEMI)/  
Université M'Hamed Bougara de Boumerdes, 35000 Boumerdes, Algeria)

<sup>2</sup>(Centre de Développement des Energies Renouvelables CDER/  
Route de l'Observatoire Bouzaréah, 16340 Algiers, Algeria)

## ABSTRACT:

This paper presents the use of the first order reliability method (FORM) to analyze the reliability of solar tower power plant (STPP). The main steps of the HL-RF iteration method, used in FORM, have been developed and listed. The example of hypothetical solar tower power plant (STPP) has been introduced in this study in order to illustrate the FORM method. The developed mathematical model of hypothetical STPP example is used as limit state function of the studied system. Results indicate that FORM is more suitable to analyze the reliability of the STPP. So, FORM has the ability to correct the first proposed design, then to give new safe design.

*Keywords - First order reliability method, design optimization, Solar Tower Power Plant*

## 1. INTRODUCTION

In engineering design, the traditional deterministic design reliability model has been successfully applied to systematically reduce the failure probability and improve quality. However, the existence of uncertainties in either engineering simulations or manufacturing processes calls for a probabilistic reliability model (PRM) for reliable and safe designs [1-4].

The study of structural and mechanical reliability is concerned with the calculation and prediction of the probability of limit-state violations at any stage during a system's life. The probability of the occurrence of an event such as a limit-state violation is a numerical measure of the chance of its occurring. Once the probability is determined, the next goal is to choose design alternatives that improve system reliability and minimize the risk of failure.

The most methods used to assess the structural and mechanical reliability and safety are: the first order reliability method (FORM) [5-8] and the second order reliability method (SORM) [9].

In the field of CSP systems, much fewer references discuss the STPP reliability evaluation [10]; after all, the STPP reliability is very important. To this end, STPP reliability analysis is developed in this work in order to evaluate the reliability and failure probability of the system. In this study, first order reliability method (FORM) has been treated. Therefore, detailed analysis of FORM has been presented in this study. An example of hypothetical STPP has been provided to illustrate this method.

## 2. DESCRIPTION OF THE SOLAR THERMAL POWER TOWER PLANT (STPP)

As shown in **Fig. 1**, the solar thermal power tower plant under consideration consists mainly of a heliostat field subsystem, a central receiver subsystem, a steam generator subsystem and a power cycle subsystem. In this study, the receiver is of a cavity receiver type and the heat transfer fluid (HTF) is a molten salt of composition 60% NaNO<sub>3</sub> and 40% KNO<sub>3</sub>.

In this plant, solar energy is collected by heliostats that reflect solar energy to a single receiver atop of a tower. The enormous amount of energy focused on the receiver is used to generate a high temperature to heat a molten salt (HTF). By mean of the molten salt, the heat absorbed by the receiver is transferred to the steam generator subsystem. The temperature of the molten salt at the receiver is of the order of 565 °C.

In the steam generator subsystem, the working fluid, which is water, is pumped at a temperature of 239 °C. In the steam generator, water absorbed the heat transferred by the HTF leading to the generation of superheated steam. The temperature of this superheated steam is of the order 552 °C. It is this steam that is used to drive the turbine generator for electricity production.

After going through the steam generator, the molten salt temperature drops to 290 °C. It is then pumped back to the receiver to start the next thermal cycle [11]. The main design characteristics considered in the present work are reported in **Table 1**.



$$\mu_{x_i}^e = x_i^* - \Phi^{-1} \left[ F_{x_i} (x_i^*) \right] \sigma_{x_i}^e \quad (3)$$

Where,  $f_{x_i}(x_i^*)$  and  $F_{x_i}(x_i^*)$  are the probability density function and the marginal cumulative function respectively, at the MPP point.

**Step 3:** Compute the safety index  $\beta$  using **Eq. (4)** and the direction cosine or sensitivity factor from **Eq. (5)**.

$$\hat{O}P^* = \beta = \frac{g(U^*) - \sum_{i=1}^n \frac{\partial g(U^*)}{\partial x_i} \sigma_{x_i} u_i^*}{\sqrt{\sum_{i=1}^n \left( \frac{\partial g(U^*)}{\partial x_i} \sigma_{x_i} \right)^2}} \quad (4)$$

The direction cosine of the unit outward normal vector is given as:

$$\begin{aligned} \cos \theta_{x_i} = \cos \theta_{u_i} &= - \frac{\frac{\partial g(U^*)}{\partial x_i}}{\left| \nabla g(U^*) \right|} \\ &= - \frac{\frac{\partial g(X^*)}{\partial x_i} \sigma_{x_i}}{\left[ \sum_{i=1}^n \left( \frac{\partial g(X^*)}{\partial x_i} \sigma_{x_i} \right)^2 \right]^{\frac{1}{2}}} = \alpha_i \end{aligned} \quad (5)$$

Where  $\alpha_i$  expresses the relative effect of the corresponding random variable on the total variation. Thus, it is called the *sensitivity factor*.

The initial  $\beta$  is computed using the mean-value method (Cornell safety-index):  $\beta = \mu_{g_a} / \sigma_{g_a}$

**Step 4:** Compute a new design point  $X_k$  and  $U_k$  (**Eqs (6) and (7)**), function value, and gradients at this new design point.

$$u_i^* = \frac{x_i^* - \mu_{x_i}}{\sigma_{x_i}} = \hat{O}P^* \cos \theta_{x_i} = \beta \alpha_i \quad (6)$$

$$x_i^* = \mu_{x_i} + \beta \sigma_{x_i} \alpha_i, \quad (i = 1, 2, \dots, n) \quad (7)$$

**Step 5:** Calculate the failure probability.

The probability of failure based on the FORM can be estimated as **Eq (8)**:

$$P_f = \Phi(-\beta) \quad (8)$$

#### 4. SIMULATION RESULTS AND DISCUSSION

The iteration results are summarized in **Table 2**. The safety-index  $\beta$  is 1.9899. Since the limit-state function value at MPP ( $T_{re,sur} = 569.3662$ ,  $\dot{m}_{st} = 3.2336$ ,  $A_{re,sur} = 0.7442$ ,  $\lambda_{tube} = 23.3876$ ) is close to zero compared to the starting value, this safety-index can be considered as the shortest distance from the origin to the limit-state surface. The new design point at MPP is the optimal design parameters ensuring the objective function ( $F_{up} = 20\%$ ).

In order to investigate the variation of the probability of failure, we must vary the unsatisfactory performance factor ( $F_{up}$ ) from 0.1 to 0.9 following the same HL-RF algorithm procedure mentioned previously.

**Table 2:** HL-RF iteration results for STPP example

<i>Iteration number</i>	<i>1</i>	<i>2</i>	<i>3</i>	<i>4</i>	<i>5</i>	<i>6</i>	<i>7</i>
$g(X_k) \times 10^7$	0.3741	-0.7365	1.1570	0.0040	0.0001	-0.0000	-0.0000
$\nabla g(T_{re,sur}) \times 10^4$	1.0611	0.0260	1.3286	0.7671	0.7743	0.7734	0.7734
$\nabla g(\dot{m}_{st}) \times 10^6$	-2.3456	-2.3782	-1.8585	-2.3582	-2.3588	-2.3588	-2.3588
$\nabla g(A_{re,sur}) \times 10^7$	1.0877	0.0337	1.2792	1.0166	1.0333	1.0333	1.0334
$\nabla g(\lambda_{tube}) \times 10^5$	4.5099	3.3721	4.6387	3.2053	3.2644	3.2613	3.2612
$\beta$	1.9064	-8.0096	1.9997	1.9894	1.9899	1.9899	1.9899
$\alpha_{T_{re,sur}}$	-0.3244	-0.0190	-0.3588	-0.2579	-0.2569	-0.2566	-0.2566
$\alpha_{\dot{m}_{st}}$	0.3585	0.8689	0.2510	0.3964	0.3912	0.3913	0.3913
$\alpha_{A_{re,sur}}$	-0.8312	-0.0616	-0.8637	-0.8545	-0.8570	-0.8571	-0.8571
$\alpha_{\lambda_{tube}}$	-0.2746	-0.4908	-0.2495	-0.2146	-0.2157	-0.2155	-0.2155
$T_{re,sur2}$ °C	562.8977	609.1404	556.9489	569.2148	569.3317	569.3644	569.3662
$\dot{m}_{st2}$ kg/s	3.2050	0.9121	3.1506	3.2366	3.2336	3.2336	3.2336
$A_{re,sur2}$ m <sup>2</sup>	0.7623	1.0740	0.7409	0.7450	0.7442	0.7442	0.7442
$\lambda_{tube2}$ W/m K	0.7623	28.5974	23.3038	23.3897	23.3871	23.3876	23.3876
$u_{T_{re,sur2}}$	-0.6184	0.1523	-0.7175	-0.5131	-0.5111	-0.5106	-0.5106
$u_{\dot{m}_{st2}}$	0.6834	-6.9596	0.5018	0.7887	0.7785	0.7786	0.7786
$u_{A_{re,sur2}}$	-1.5846	0.4935	-1.7272	-1.7000	-1.7053	-1.7055	-1.7055
$u_{\lambda_{tube2}}$	-0.5234	3.9309	-0.4989	-0.4270	-0.4292	-0.4288	-0.4288
$\varepsilon$	-	5.2015	1.2497	0.0052	0.0003	0.0000	0.0000

**Fig. 2** shows the probability of failure function or cumulative distribution function (CDF) of the unsatisfactory performance factor ( $F_{up}$ ). This plot can be used to predict the probability of  $F_{up}$  being less (or more) than a particular value, or between two values. For example, in this graph, there is approximately a 60 % probability that  $F_{up}$  will be less than 50 % and 40% probability that  $F_{up}$  will be greater than 50 %. There is approximately a  $0.6 - 0.1 = 0.5$  (50%) probability that  $F_{up}$  will be between 30 % and 50 %. In other words, the probability of risk (40%) is too high so it is important to decrease this probability. In this case we must know the design parameter influencing on this probability. To this end it is necessary to analyze the sensitivity factor  $\alpha$ , the parameter representing the high sensitivity factor is the parameter which has a great influence. In this example the receiver surface area  $A_{re,sur}$  is the parameter having the highest sensitivity factor  $(\alpha_{A_{re,sur}})^2 = 0,7346$ .

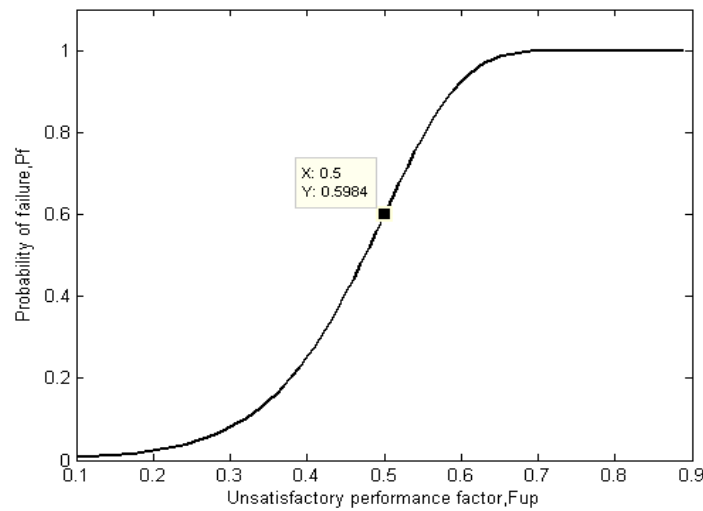


Fig. 2 – Failure function of the STPP unsatisfactory performance factor for  $A_{re,sur} = 1 \text{ m}^2$

The **Fig. 3** another simulation example where  $A_{re,sur} = 0.9 \text{ m}^2$  in the initial design point. We notice that, there is approximately 80 % probability that  $F_{up}$  will be less than 50 % and 20% probability that  $F_{up}$  will be greater than 50 %. So in this case the probability of risk is decreased by 20%.

We can also reduce the probability of risk by modifying the parameters which represent the following sensitivity factor in decreasing order.  $(\alpha_{\dot{m}_{st}})^2 = 0.1531$  and  $(\alpha_{T_{re,sur}})^2 = 0.0658$  are the following sensitivity factors in decreasing order, but practically we cannot modify these two parameters ( $\dot{m}_{st}$  and  $T_{re,sur}$ ) because  $\dot{m}_{st}$  is related to the consumption (output energy) and  $T_{re,sur}$  related to the solar energy (input energy). Therefore, the only parameter can be changed is  $\lambda_{tube}$ .

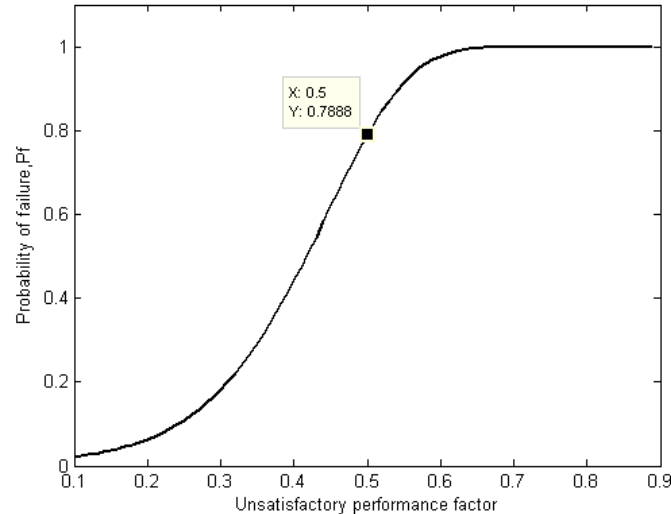


Fig. 3 – Failure function of the STPP unsatisfactory performance factor for  $A_{re,sur} = 0.9 \text{ m}^2$

**Fig. 4** shows the Probability of failure function of the STPP unsatisfactory performance factor for  $A_{re,sur} = 0.9 \text{ m}^2$  and  $\lambda_{tube} = 23 \text{ W/m.K}$ . We notice that, there is approximately 85 % probability that  $F_{up}$  will be less than 50 % and 15% probability that  $F_{up}$  will be greater than 50 %. So in this case the probability of risk is decreased by 25% than the first case ( $A_{re,sur} = 1 \text{ m}^2$  and  $\lambda_{tube} = 23.9 \text{ W/m.K}$ ).

The graph of Fig. 5 shows the variation of the reliability function ( $R = 1 - F$ ) with the variation of unsatisfactory performance factor  $F_{up}$ . When  $F_{up}$  increases, the reliability of STPP decreases (when  $F_{up} \leq 10\%$ ,  $R = 1$  and when  $F_{up} \geq 70\%$ ,  $R = 0$ ). Physically, the reliability of any system decrease when there is loss of performances.

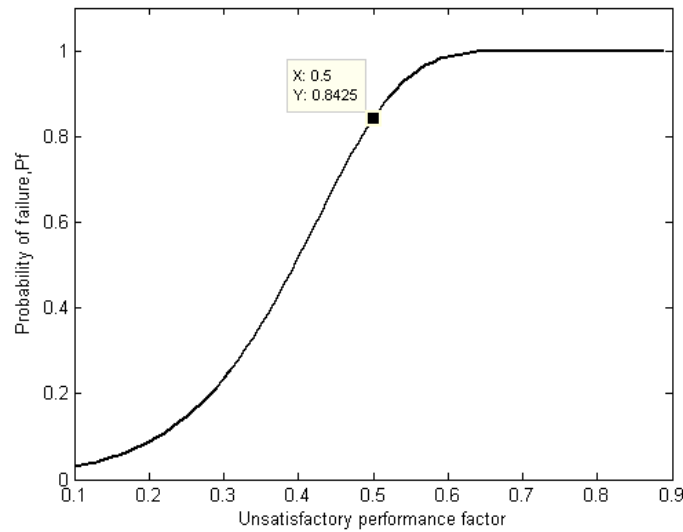


Fig. 4 – Probability of failure function of the STPP unsatisfactory performance factor for  $A_{re,sur} = 0.9 \text{ m}^2$  and  $\lambda_{tube} = 23 \text{ W/m.K}$

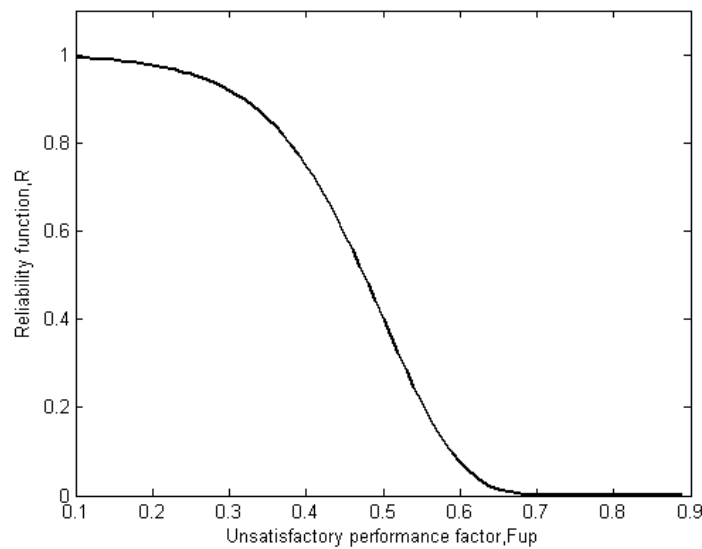


Fig. 5 – Reliability function of the STPP unsatisfactory performance factor for  $A_{re,sur} = 1 \text{ m}^2$

The different optimal safe designs with the variation of  $F_{up}$  are summarized in **Table 3**. When  $F_{up}$  increases,  $T_{re,sur}$ ,  $A_{re,sur}$  and  $\lambda_{tube}$  increase. Indeed, the augmentation of the receiver surface temperature and the receiver surface area generates higher heat losses by reflection and emission. However, the augmentation of the tube conductivity causes higher conductive heat losses. In the other hand, the steam mass flow  $\dot{m}_{st}$  decreases when  $F_{up}$  increases. The steam mass flow is used to calculate the net output energy given by the receiver. When  $F_{up}$  increases, an important part the absorbed receiver energy will be lost (energy losses). Therefore, the net output energy from the receiver will be reduced ( $\dot{m}_{st}$  decreases).

**Table 3:** Different optimal safe designs with the variation of  $F_{up}$ 

$F_{up}$	10%	20%	30%	40%	50%	60%	70%	80%	90%
$g(X_k) \times 10^7$	0.0000	-0.0000	-0.0000	0.0000	-0.0000	-0.0000	0.0000	0.0000	0.0000
$\nabla g(T_{re,sur}) \times 10^4$	0.7852	0.7734	0.7547	0.7262	0.6840	0.6217	0.5290	0.3878	0.1798
$\nabla g(\dot{m}_{st}) \times 10^6$	-2.3590	-2.3588	-2.3583	-2.3576	-2.3565	-2.3544	-2.3505	-2.3408	-2.2986
$\nabla g(A_{re,sur}) \times 10^7$	1.1529	1.0334	0.9159	0.8001	0.6848	0.5678	0.4446	0.3073	0.1475
$\nabla g(\lambda_{tube}) \times 10^5$	3.3068	3.2612	3.1889	3.0778	2.9103	2.6581	2.2730	1.6691	0.75862
$\beta$	2.4731	1.9899	1.4005	0.6708	-0.2491	-1.4336	-2.9959	-5.0866	-7.7077
$\alpha_{T_{re,sur}}$	-0.2395	-0.2566	-0.2736	-0.2895	-0.3022	-0.3083	-0.3004	-0.2602	-0.1462
$\alpha_{\dot{m}_{st}}$	0.3598	0.3913	0.4275	0.4699	0.5205	0.5837	0.6673	0.7853	0.9346
$\alpha_{A_{re,sur}}$	-0.8791	-0.8571	-0.8302	-0.7973	-0.7564	-0.7038	-0.6312	-0.5155	-0.2999
$\alpha_{\lambda_{tube}}$	-0.2009	-0.2155	-0.2303	-0.2443	-0.2561	-0.2625	-0.2570	-0.2231	-0.1229
$T_{re,sur2}$ °C	564.461	569.3662	577.0068	588.3495	604.5163	626.5158	653.9945	679.4207	667.6276
$\dot{m}_{st2}$ kg/s	3.2669	3.2336	3.1796	3.0946	2.9611	2.7490	2.4003	1.8016	0.8388
$A_{re,sur2}$ m <sup>2</sup>	0.6739	0.7442	0.8256	0.9198	1.0283	1.1514	1.2836	1.3933	1.3468
$\lambda_{tube2}$ W/m K	23.3063	23.3876	23.5146	23.7041	23.9762	24.3497	24.8202	25.2559	25.0317
$u_{T_{re,sur2}}$	-0.5923	-0.5106	-0.3832	-0.1942	0.0753	0.4419	0.8999	1.3237	1.1271
$u_{\dot{m}_{st2}}$	0.8897	0.7786	0.5988	0.3152	-0.1297	-0.8368	-1.9991	-3.9947	-7.2040
$u_{A_{re,sur2}}$	-2.1741	-1.7055	-1.1628	-0.5348	0.1884	1.0090	1.8910	2.6223	2.3117
$u_{\lambda_{tube2}}$	-0.4968	-0.4288	-0.3225	-0.1639	0.0638	0.3763	0.7701	1.1346	0.9471
$\varepsilon$	0.0000	0.0000	0.0000	0.0000	0.0000	0.0000	0.0000	0.0000	0.0000

## 5. CONCLUSION

The main steps of the HL-RF iteration method, used in FORM, have been developed and listed. The example of hypothetical STPP has been introduced in this study in order to illustrate the FORM method. The developed mathematical model of hypothetical STPP example is used as limit state function of the studied system. Receiver surface temperature ( $T_{re,sur}$ ), steam mass flow ( $\dot{m}_{st}$ ), receiver surface area ( $A_{re,sur}$ ) and tube conductivity ( $\lambda_{tube}$ ) have been used as the random variables in the limit state function. In the same time,  $T_{re,sur}$ ,  $\dot{m}_{st}$ ,  $A_{re,sur}$  and  $\lambda_{tube}$  are the coordinates of the wanted most probable point (MPP). Unsatisfactory performance factor  $F_{up}$  is used as the objective condition in the limit state function. After seven iteration the limit-state function value at MPP ( $T_{re,sur} = 569.3662$ ,  $\dot{m}_{st} = 3.2336$ ,  $A_{re,sur} = 0.7442$ ,  $\lambda_{tube} = 23.3876$ ) is close to zero. This point at MPP is considered as the new design point. The graphs representing the variation of the probability of failure and the reliability function versus  $F_{up}$ , for different values of  $A_{re,sur}$ , have been commented.

In the basis of these results we can conclude that the FORM seems suitable to analyze the reliability of the STPP and it can be used as a guide to identify the most probable point (MPP). So, FORM has the ability to correct the first proposed design, then to give new safe design.

## 6. REFERENCES

- [1] Clifford K. Ho & Gregory J. Kolb. Incorporating Uncertainty into Probabilistic Performance Models of Concentrating Solar Power Plants. *Journal of Solar Energy Engineering*, 2010, Vol. 132 / 031012.
- [2] Clifford K. Ho, Siri S. Khalsa, Gregory J. Kolb. Methods for probabilistic modeling of concentrating solar power plants. *Solar Energy*, 85 (2011) 669–675.
- [3] Henrik Stensgaard Toft, John Dalsgaard Sørensen. Reliability-based design of wind turbine blades. *Structural Safety* 33 (2011) 333–342.
- [4] André Teófilo Beck, Wellison José de Santana Gomes. A comparison of deterministic, reliability-based and risk-based structural optimization under uncertainty. *Probabilistic Engineering Mechanics* 28 (2012) 18–29.
- [5] V. Verderaiame. Illustrated structural application of universal first-order reliability method. NASA Technical Paper 3501, August 1994.
- [6] Y.K. Wen. Reliability and performance-based design. *Structural Safety* 23 (2001) 407– 428.
- [7] Irfan Kaymaz, Kurt Marti. Reliability-based design optimization for elastoplastic mechanical structures. *Computers and Structures* 85 (2007) 615–625.
- [8] Jinsong Huang, D.V. Griffiths. Observations on FORM in a simple geomechanics example. *Structural Safety*, 33 (2011) 115–119.
- [9] Yan-Gang Zhao, Tetsuro Ono. A general procedure for first/second-order reliability method (FORM/SORM). *Structural Safety* 21 (1999) 95-112.
- [10] Benammar S, Khellaf A, Mohammedi K. Solar tower power plants performance and reliability analysis. In: solar power, Editor: Stephen Bailey. Nova science publishers, Inc. ISBN: 978-1-63321-317-3. USA, 2014b.
- [11] Falcone PK. A Handbook for Solar Central Receiver Design, Sandia National Laboratories, Livermore, CA. December, 1986. Report SAND 86-8009.
- [12] Benammar S, Khellaf A, Mohammedi K. Contribution to the modeling and simulation of solar power tower plants using energy analysis. *Energy Conversion and Management*, 2014a, 78, 923–930.
- [13] Rackwitz, R & Fiessler, B. Structural reliability under combined load sequences. *Computers and Structures*, 1978, 9(8), 489–494.
- [14] Santosh TV; Saraf RK; Ghosh AK & Kushwaha HS., Optimum step length selection rule in modified HL-RF method for structural reliability. *International journal of Pressure Vessels Piping*, 2006, 83(10), 742–748.
- [15] Keshtegar B. and Miri M. An Enhanced HL-RF Method for the Computation of Structural Failure Probability Based On Relaxed Approach. *Civil Engineering Infrastructures Journal*, 2013, 46 (1): 69 – 80, ISSN: 2322 – 2093.
- [16] Choi SK, Grandhi RV, Canfield RA. Reliability-based structural design, Springer-Verlag, London (2007).
- [17] Keshtegar B. and Miri M. Reliability analysis of corroded pipes using conjugate HL-RF algorithm based on average shear stress yield criterion. *Engineering Failure Analysis* 46 (2014) 104-117.